

SPATIAL PATTERNS OF VINEYARD LANDSCAPE EVOLUTION AND THEIR IMPACTS ON EROSION SUSCEPTIBILITY: RUSLE SIMULATION APPLIED IN MERCUREY (BURGUNDY, FRANCE) SINCE THE MID-20TH CENTURY

ETIENNE COSSART, MATHIEU FRESSARD and BRIAN CHAIZE

With 14 figures and 2 tables

Received 23 December 2020 · Accepted 11 January 2021

Summary: Erosion susceptibility in vineyards is approximately one order of magnitude above the reference level calculated for all agricultural activities, and preventing soil erosion is thus one of the most important environmental issues in vineyards. Spatially explicit models are necessary to address the coevolution of erosion susceptibility and anthropogenic practices because of the heterogeneous spatial patterns of erosion within vineyards. In this paper, we apply the RUSLE model to assess erosion susceptibility through time in a Burgundy vineyard (Mercurey) at a catchment scale (15 km²). The model is first calibrated with data acquired in 2015–2018. Second, erosion susceptibility during former stages (1953 and 1984) is compared to current reference frame. Such theoretical comparison considers that both C (land cover) and LS (Length-Slope) factors evolved through time. We hypothesize that such factors reveal both the land use evolution (especially agricultural land uses) and the development of a soil erosion management strategy based on the collection of sediments using roads, hedges and ditches. The current reference frame of erosion susceptibility calculated at catchment scale is about 9,152 t.yr⁻¹. In the early 1980s a peak in erosion susceptibility is concomitant with vineyard expansion during the second half of the 20th century. Erosion susceptibility in vine parcels in 1984 is estimated to be 32% higher than current period. In the mid-20th century the spatial patterns of agricultural land use (patchwork of grasslands and vines, vines on moderately-rugged hillslopes) led to moderate rates of erosion susceptibility. At this stage, past level of erosion susceptibility is estimated to be 40% lower than current reference frame.

Zusammenfassung: Die Erosionsanfälligkeit in Weinbaugebieten liegt etwa eine Größenordnung über dem für alle landwirtschaftlichen Aktivitäten berechneten Referenzwert, und die Verhinderung von Bodenerosion ist daher eines der wichtigsten Umweltthemen im Weinbau. Räumlich explizite Modelle sind notwendig, um das Zusammenwirken von Erosionsanfälligkeit und anthropogenen Praktiken aufgrund der heterogenen räumlichen Muster der Erosion in Weinbauflächen zu berücksichtigen. In dieser Arbeit wenden wir das RUSLE-Modell an, um die Erosionsanfälligkeit im Laufe der Zeit in einem burgundischen Weinbauareal (Mercurey) auf Einzugsgebietsebene (15 km²) zu bewerten. Das Modell wird zunächst mit Daten aus den Jahren 2015–2018 kalibriert und in einem zweiten Schritt wird die Erosionsanfälligkeit während früherer Phasen (1953 und 1984) mit dem aktuellen Referenzrahmen verglichen. Dieser theoretische Vergleich berücksichtigt, dass sich sowohl Landbedeckung als auch topographische Faktoren im Laufe der Zeit verändert haben. Wir stellen die Hypothese auf, dass diese Faktoren sowohl die Entwicklung der Landnutzung (insbesondere der landwirtschaftlichen Nutzung) als auch die Entwicklung einer Bodenerosionsmanagementstrategie, welche auf der Sammlung von Sedimenten durch Straßen, Hecken und Gräben basiert, aufzeigen. Der aktuelle Bezugsrahmen der auf Einzugsgebietsebene berechneten Erosionsanfälligkeit beträgt etwa 9.152 t.yr⁻¹. Der Höhepunkt der Erosionsanfälligkeit in den frühen 1980er Jahren geht mit der Ausweitung der Weinbaufläche in der zweiten Hälfte des 20. Jahrhunderts einher. Die Erosionsanfälligkeit in den Weinbauparzellen wird für 1984 auf 32 % höher als in der aktuellen Periode geschätzt. In der Mitte des 20. Jahrhunderts führten hingegen die räumlichen Muster der landwirtschaftlichen Bodennutzung (Mosaik aus Grünland und Reben, Reben auf mäßig zerklüfteten Hängen) zu moderaten Raten der Erosionsanfälligkeit. Zu diesem Zeitpunkt wird das frühere Niveau der Erosionsanfälligkeit auf 40 % niedriger als der aktuelle Bezugsrahmen geschätzt.

Keywords: erosion, soil, vineyard, RUSLE, Burgundy

1 Introduction

World-renowned French vineyards are the result of a centuries-old historical evolution. Since the Roman period, both the spatial extent of vineyards and the practices in terms of wine-growing have significantly changed under the combined effects of

cultural, social, economic and environmental factors (LAMMOGLIA et al. 2018). Among all parameters that drive this complex evolution, soil is of prime importance because it defines the quality of wine terroirs and thus influences the economic added value of wines (VAUDOUR 2002). However, it is well known that the local physical settings of vineyards

(i.e., soil grain size, organic matter content and slope gradient) and the specific cultivation practices used (such as tillage and slope-oriented rows) make wine-growing soils particularly prone to denudation (BLAVET et al. 2009; RODRIGO-COMINO 2018). The erosion susceptibility is approximately one order of magnitude above the reference level calculated for all agricultural activities (CERDAN et al. 2006).

For instance, in French vineyards, average current erosion rates range from 10.5 to 54 t·ha⁻¹·yr⁻¹ (QUIQUEREZ et al. 2008; BRENOT et al. 2008; PAROISSIEN et al. 2010; PROSDOCIMI et al. 2016; FRESSARD et al. 2017). As a consequence, preventing soil erosion is one of the most important environmental issues in vineyards. This issue is well perceived by wine growers who have coped with soil losses since the Middle Age, especially in Burgundy (GARCIA et al. 2018; LABBÉ and GARCIA 2019).

However, vineyards are characterized by a wide range of anthropogenic practices and complex landscape structures, generating high local variability in terms of erosion processes and denudation rates (FOLLAIN et al. 2012; BIDDOCU et al. 2014; BAGAGIOLO et al. 2018). Due to such spatial heterogeneity, we thus still face a lack of knowledge to decipher the efficiency of mitigation strategies on soil erosion over time. Sedimentary signals interpreted from sedimentary archives are indeed of insufficient resolution to depict the coevolution of erosion susceptibility with anthropogenic practices through historic periods (LARUE et al. 1999; LARUE 2001). More specifically, models undertaking broad-scale assessments of soil erosion should take into account the broad-scale dynamics of land use change (BAKKER et al. 2008; CIAMPALINI et al. 2012; DAVID et al. 2014).

In this paper, we seek to calibrate a spatially explicit model (Revised Universal Soil Loss Equation, RUSLE in WISCHMEIER and SMITH 1965) to assess current erosion susceptibility in a vineyard. Here, we focus on the Giroux catchment where the Mercurey terroir (Burgundy, France) is located. From a historical survey (aerial photographs and interviews with vine growers), we reconstructed landscape evolution since 1950 at the catchment scale. Two complementary dates representative of vineyard history were selected: 1953 corresponds to the beginning of post-World War economic growth, 1984 corresponds to the paroxysmal period of wine growing. Specific attention is paid to agricultural land use, urban sprawl and manmade infrastructure networks (e.g., roads, hedges, and ditches). Such data are implemented within a spatio-temporal GIS to compare past ero-

sion susceptibility with the current reference state. The results exhibit the evolution of soil prevention strategies since the mid-20th century and, more generally, may contribute to the discussion of their efficiency.

2 Study Area

2.1 Physical settings

We focus on the Giroux catchment (13.91 km²) where the vineyards of Mercurey (640 ha) are located (Côte-de-Bourgogne, Burgundy, France). The Côte-de-Bourgogne (i.e., from the Côte-de-Nuits in the north to the Côte-Chalonnaise in the south) is a structural escarpment set on a NNE-SSW fault line that subdivides the Morvan massif (horst) and the Saône floodplain (graben). The hillslope morphology is very similar throughout the escarpment (Fig. 1) and is characterized by an Oxfordian limestone rock wall at the top (whose height ranges from 20 to 70 meters) and a well-shaped concave profile at the bottom (Oxfordian marl or marly limestones) (MÉRIAUX et al. 1981).

The Giroux catchment is set in an atypical structural pattern within the region. The fault system between the Morvan horst and the Saône graben is complex, as six main faults create a set of tilted blocks, in which the roof tends to drop from west to east. Guided by these weak lines, differential erosion shaped a wide catchment (5 kilometers long, 3 kilometers wide), which is characterized by compactness (Gravelius index = 1.2). The basin is subdivided into 8 main subbasins, and geometrical patterns favor the convergence of waters through the village of Mercurey (Fig. 2) (FRESSARD et al. 2017). In detail, the hillslope height is approximately 110 to 130 meters, and the length ranges from 1 to 1.5 km. The slope gradients reach 25° to 35° in the upper part of the hillslopes (limestone ledge) and gradually decrease near the thalweg where the slope gradient is less than 3° (Fig. 2).

Precipitation patterns are characteristic of transitional areas between maritime and continental climates. The average precipitation value is 770 mm·year⁻¹ measured at the amateur weather station of Mercurey (since 1971). The seasonal pattern is characterized by higher precipitation values in August and September (80 mm) because of storm events and associated intense rainfall: 14 of the 18 storm events recorded from 1971 to 2018 (>50 mm in one day) occurred during these two months.

Most of the Mercurey soils are brown calcareous or calcic soils developed on limestone and marls. Thicker soils developed on colluvial deposits can be observed in the valley bottoms (SIGALES 2007). Their texture is fine to very fine and characterized by a high clay content, as most of the samples are between 35 and 50% clay (Fig. 3). These soils exhibit a sufficient organic matter (OM) content for vineyard-cultivated soils ($\pm 2\%$ of OM over the area) and a basic pH due to their calcareous origin.

2.2 History and environmental issues

As in all Burgundy terroirs, maintaining the quality of the soil resource is one of the major environmental issues in Mercurey. The soil is indeed a very important part of the classification system of Burgundy's wine appellations (GARCIA 2011). For this reason, modifying the local soil characteristics of each vineyard plot is strictly forbidden. As a result, the loss of soil is irreversible, and compensation by artificial allochthonous soil inputs is strictly forbidden. Winegrowers have thus coped with soil erosion. As early as the 9th and 13th centuries, they developed strategies to reduce denudation rates or to collect sediments within the plots before the sediments were exported from the catchment area (GARCIA 2011). At that time, stone structures were built to increase surface roughness, causing soil particle impoundment (BRENOT 2007). In the 17th-18th centuries, while the vineyard gradually spread and vines started to be grown on the hillslopes, networks of dry stone walls and vegetated hedges were built. The axes of these infrastructures are perpendicular to the highest slope gradient so that they impede sedimentary flows. Dry stone walls as well as hedges are permeable and act as sieves: water passes through while sediments are trapped. Gathered sediments are then transferred manually to erosion scars to compensate for soil losses (GARCIA et al. 2018; LABBÉ and GARCIA 2019).

After the successive crises of phylloxera (late 19th century), mildew (early 20th century) and a number of climatic hazards (hail in 1927 and 1928, frost in 1930 and 1932), the wine system collapsed in Mercurey: only 310 hectares were still cultivated in 1940 (GRIVOT 1954). After the Second World War, the Mercurey vineyard (as everywhere in Burgundy) experienced a phase of economic growth that implied a significant spread of vineyards, so that most of grassland parcels were converted into vines (Fig. 4). The surface area reached 860 hectares at the end of the 20th century (AGRESTE 2000).

During this recent period, two flash floods occurred in 1981 and 1983, so collective awareness emerged. The hydrometeorological event of August 10, 1981, is indeed a reference by the level of rainfall (119.5 mm of rain in 24 hours) but also by the total amount of damage (destroyed roads, approximately forty flooded houses, the product of previous harvests destroyed, etc.). As a consequence, the owners of the Mercurey appellation created an association to collectively manage vineyard maintenance, especially in terms of soil erosion and flash flood pre-

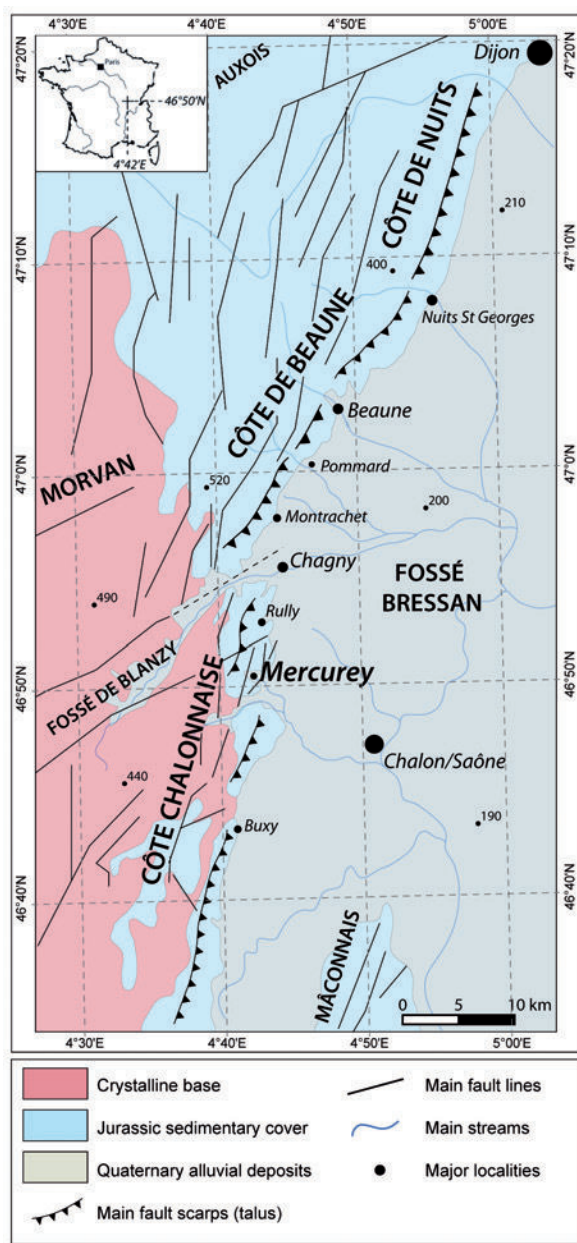


Fig. 1: Geomorphological sketch of the Burgundy coast. Source: Bureau des Recherches Géologiques et Minières (BRGM).

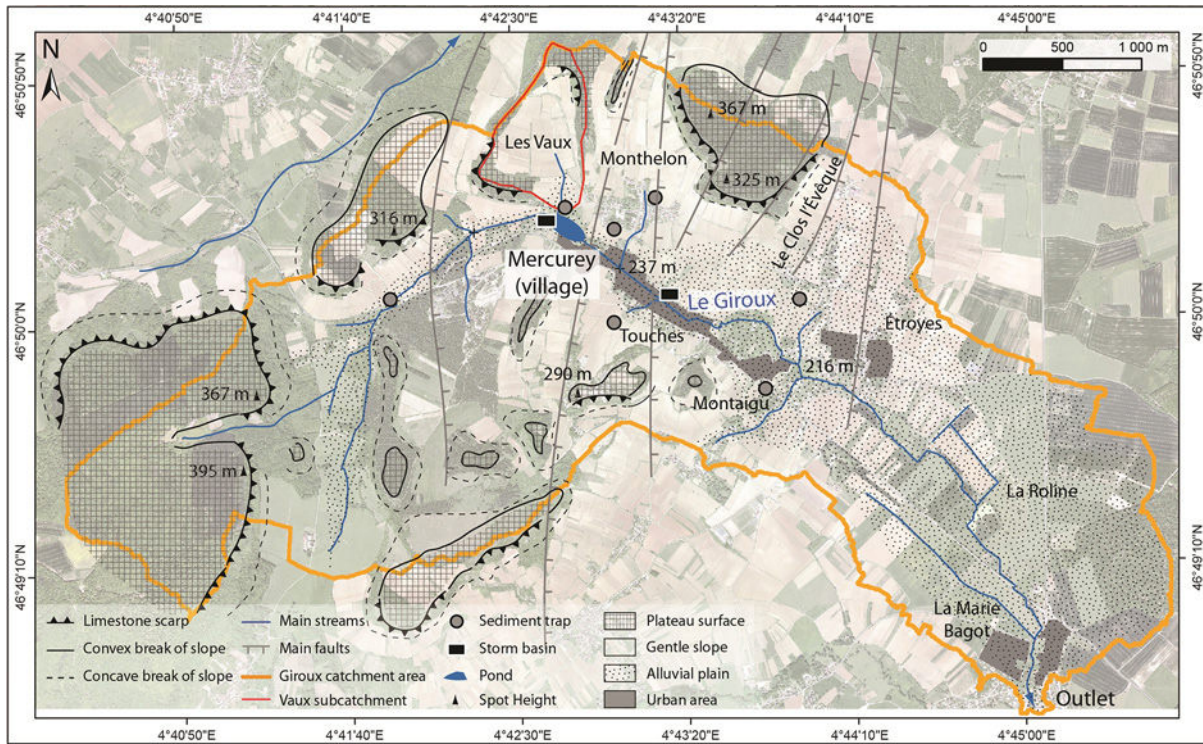


Fig. 2: Geomorphological sketch of the Giroux catchment (background aerial image, IGN 2013)

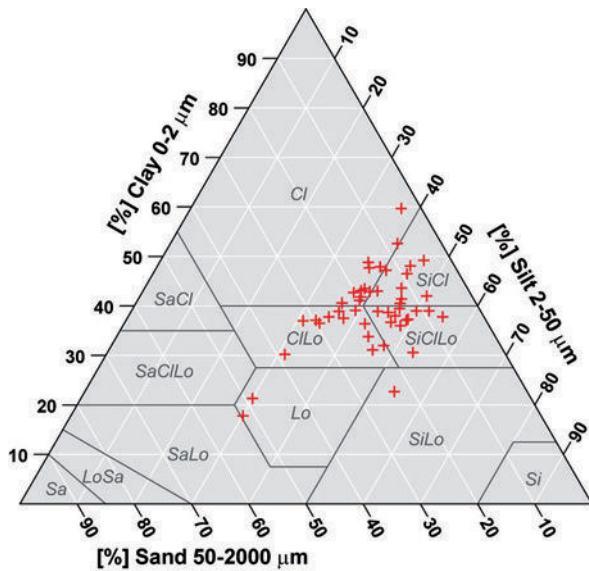


Fig. 3: Soil texture triangle of the Mercurey area using the USDA soil classification. Cl = clay, SiCl = silty clay, SaCl = sandy clay, ClLo = clay loam, SiClLo = silt clay loam, SaClLo = sandy clay loam, Lo = loam, SiLo = silty loam, SaLo = sandy loam, Si = silt, LoSa = loamy sand, Sa = sand. (data obtained from Sigales, 2007). Locations of the soil samples are shown in Fig. 7.

vention. During the 1980s, they first simplified the spatial pattern of parcels by regrouping it. Second, they created a new network of hydraulic infrastruc-

tures to collect sediments removed from the plots before they are exported to the river. A complex assemblage of transverse paths on hillslopes and v-shaped paths along thalwegs was designed by the CEMAGREF of Lyon (currently INRAE) between 1988 and 1995. Additionally, several storage basins were constructed to limit the flood peaks and protect the inhabited valley bottoms in the case of rainstorms. The infrastructures have deeply modified sediment connectivity, as sediments exported from hillslopes are impeded, while sediments reaching thalwegs are directly transferred into sinks (FRESSARD and COSSART 2019). This strategy reactivates the former anthropogenic soil backfill system.

3 Methods

3.1 Current reference frame of erosion susceptibility

3.1.1 RUSLE model parameterization

In vineyards, the geometry of paths, furrows, ditches and hedges generates high overland heterogeneity and nonlinearity between the sediment supply at the plot scale and the sediment yield at the

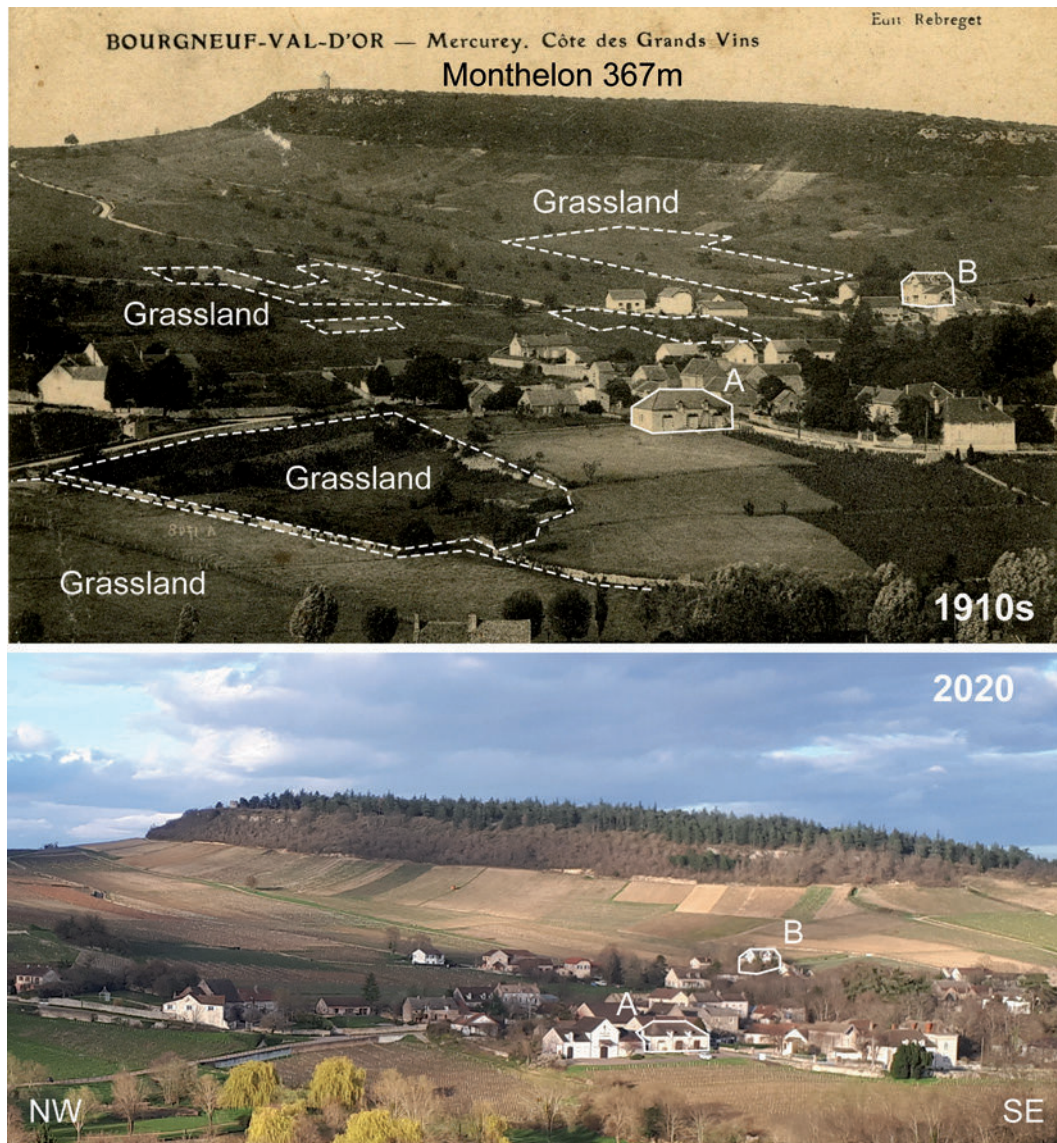


Fig. 4: Modification of land cover in Mercurey Vineyard. Up: Historical postcard of Mercurey, view of the Bourgneuf-Val-d'Or area dated from 1910 (source: department archives). Note the density of trees and the land use patchwork on hillslopes. Down: Photograph acquired in march 2020 (by Etienne Cossart), note the homogeneous land use (vineyard). Two houses are highlighted (A and B) to make the comparison through time easier.

catchment scale (RACLOT et al. 2009). Erosion susceptibility mapping at the catchment scale is thus required to consider the spatial patterns of soil erosion, especially by taking into account natural or artificial factors that affect hydrological connectivity (e.g., landscape structure, location of manmade infrastructures) (BAKKER et al. 2008; LEDERMANN et al. 2010). Furthermore, the catchment is the operational scale at which management actions and operations focus (SCHULZE 2000), so it is a suitable scale to discuss the efficiency of the strategies of soil loss prevention.

Among models of erosion, the RUSLE model has been extensively applied (KINNEL 2010; JAHUN et al. 2015; RODRIGO-COMINO 2018). It is spatially explicit and can be implemented through GIS software with multisource temporal databases to determine the effects of past land use changes on erosion susceptibility (PONTE-LIRA et al. 2012; PANAGOS et al. 2015a). The predictive model based on the Universal Soil Loss Equation (USLE) (WISCHMEIER and SMITH 1965 and 1978) is:

$$A=R \times K \times L \times S \times C \times P$$

where \mathcal{A} = soil loss per area and time (in $\text{t}\cdot\text{ha}^{-1}\cdot\text{y}^{-1}$); R = a rainfall erosivity factor (in $\text{MJ}\cdot\text{mm}\cdot\text{ha}^{-1}\cdot\text{h}^{-1}\cdot\text{y}^{-1}$); K = a soil erodibility factor (in $\text{t}\cdot\text{h}\cdot\text{MJ}^{-1}\cdot\text{mm}^{-1}$); L = a slope length factor (dimensionless); S = a slope steepness factor (dimensionless); C = a cover-management factor (dimensionless); and P = a support practice factor (dimensionless).

3.1.2 Land use and C-Factor

Land use is interpreted from field survey and 2018 image, that is an orthophotograph available directly from the French National Geographic Institute IGN (BDOrtho®). We identified 6 types of land use: vineyard, grassland, other crops, shrubs, forested areas, and buildings.

Land use polygons were manually digitalized based on the visual interpretation of the aerial orthophotographs (detailed below). We implemented the RUSLE model with averaged values of C-factor inventoried from the literature (Tab. 1). The synthesis shows that the variability in the estimated C-factor is very low for forests, while it is higher in the case of both vineyards and grasslands. In detail, extreme values are calculated from remote sensing methods and NDVI-derived indices (KOULI et al. 2009; PANAGOS et al. 2015b): NDVI provides the maximal estimated value for grassland ($C = 0.54$) and a low value for vineyards ($C = 0.29$). Estimations based and calibrated from empirical surveys converge to the average values (GRIMM et al. 2003; MÄRKER et al. 2008; FAGNANO et al. 2012; RANZI et al. 2012).

In case of vineyards these values range from 0.35 to 0.45 and correspond to values suggested by ARPAV (Agenzia Regionale per la Prevenzione e Protezione Ambientale del Veneto) for 2-dimensional grape trellis system (BARRENA-GONZÁLEZ et al. 2020), a system observed in Burgundy. Average values range from 0.04 to 0.18 for grasslands. These mean values are integrated within the attribute table of the GIS layers.

3.1.3 LS Factor

The LS factor is traditionally derived from the available DEM in GIS (MOORE et al. 1991; DESMET and GOVERS 1996; KINNELL 2005). Nevertheless, directly available DEM resolutions (25 meters in France) cannot account for the fine-scale deformation of road and path networks (Fig. 5A and 5B) that have a great influence on hydrological and sedimentary connectivity (FRESSARD and COSSART 2019). From the 2018 image we made an inventory of all linear manmade infrastructures and specified to what extent they interfere with flow accumulation and flow path geometry. Following a methodological framework applied in complex agricultural landscapes (REULIER et al. 2019), stone walls and hedges are assumed to act as a sieve and may create an obstacle that modifies the flow path (divergent flow); ditches have a lower altitude than their neighboring cells so that they concentrate water flows. Roads may imply both divergent flow and flow concentration, depending on whether they are cut or filled within fields. The concomitant modification of runoff flow paths is integrated within GIS.

Tab. 1: Theoretical C values

References	KOULI et al. 2009	GANASRI and RAMESH 2016	RANZI et al. 2012	SHIT et al. 2015	BHANDARI et al. 2015	BORELLI et al. 2018	MÄRKER et al. 2008	PANAGOS et al. 2015b	BAKKER et al. 2008	Mean	St-D
	NDVI	Supervised classification	Meta analysis	Meta analysis	Field observation	Meta analysis	Meta-analysis	Statistical modelling	Field observation		
Land Use	Grèce 684km ³	India 3,128 km ³	Vietnam 38,165 km ³	India 44 km ³	Nepal 123 km ³	Europe	Italy 3,015 km ³	France	Western Europe		
Built areas		0.090	0.000	0.000	0.050	0.000	0.000	0.000	0.000	0.018	0.032
Vineyards	0.294					0.451	0.451	0.340	0.200	0.347	0.096
Grasslands	0.545		0.180		0.020	0.150	0.050	0.090	0.200	0.176	0.163
Croplands	0.428	0.630	0.500	0.400	0.450	0.138	0.200	0.258	0.026	0.337	0.182
Market gardening	0.496		0.500	0.400	0.450	0.100	0.300	0.100	0.097	0.305	0.170
Shrub	0.500		0.180	0.050	0.010	0.042	0.050	0.023	0.040	0.112	0.155
Forested areas	0.182	0.003	0.003	0.008	0.001	0.003	0.002	0.001	0.020	0.025	0.056

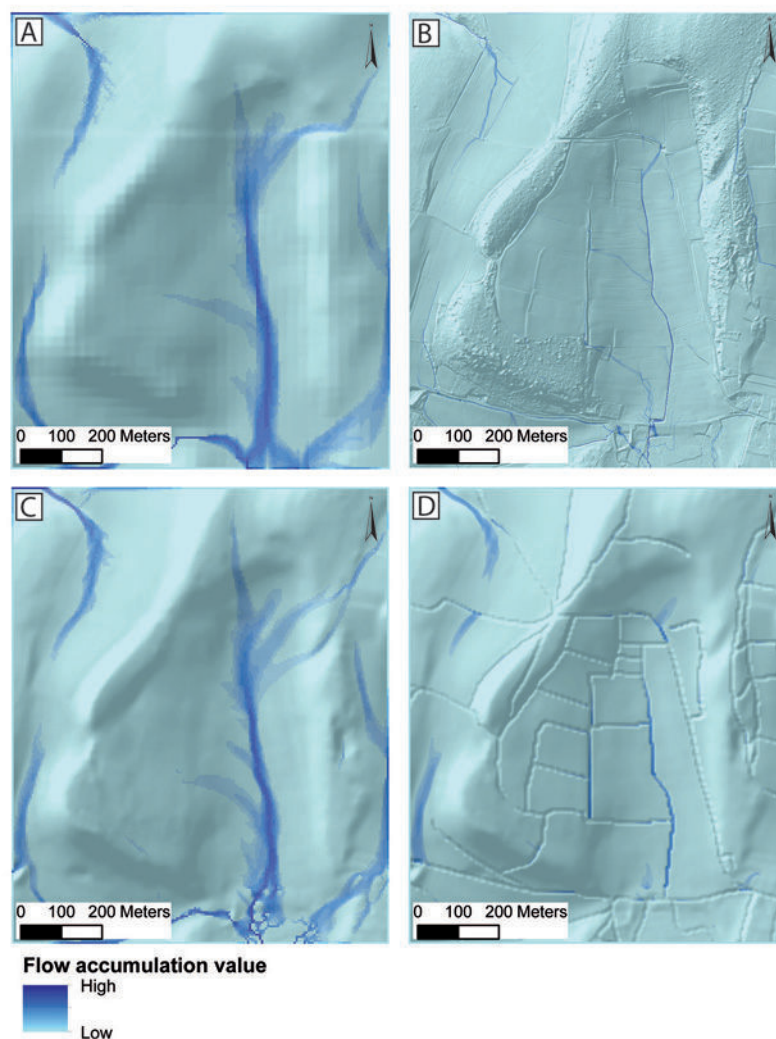


Fig. 5: Flow accumulation rasters with hillshades overlapping in transparency for the different available and derived DEMs, close-up view of the Vaux area. A = IGN 25 DEM; B=Lidar DEM; C=recreated no road DEM and D=2018 DEM with burnt roads.

To estimate LS factors that include manmade infrastructures, we first produced a high-resolution DEM that does not include the road path (initial DEM) that could be considered as a non-anthropized DEM (Fig. 5C). The main objective is to obtain a DEM at a sufficient resolution that could integrate the geometry of manmade infrastructures (roads, ditches, hedges) and their respective influence on the flow direction at the catchment scale (divergent flow vs. concentration). The initial DEM was produced using a 1 meter-resolution Lidar DEM available from the DREAL (Direction Régionale de l'Environnement, de l'Aménagement et du Logement of Burgundy) acquired in 2015. At this fine resolution, the DEM includes several roads and talus slopes that have to be corrected (removed) to produce the initial DEM.

Three types of routines have been applied (Fig. 5):

(1) Resampling: The initial 1-meter resolution has been resampled to 5 meters to smooth the artefacts observed on the land surface that might lead to fuzzy extraction of hydrological features (LI and WONG 2010). The 5 meters resolution is in accordance with the scale of the other layers (i.e., aerial photographs: 25,000 scale and soil map: 10,000 scale), considering the relationship between pixel resolution and scale (HENGL 2006).

(2) Local filtering: Local filtering has been applied within a buffer of 20 meters around roads and paths to remove local terraced shapes due to talus slopes and roads. In this case, we used the 'terrain filter' and the 'pit and bump filters' DEM editing libraries of PCI Geomatica®.

(3) Global filtering: To remove the last artefacts and smooth the DEM, the “remove noise filter” tool of PCI Geomatica® was used.

Secondly, to take into account the hydrological function of these roads and ditches, they were integrated into the DEM as stream lines so that they intercept the water and sediment flow. All road tracks and agricultural paths were digitalized. They were integrated into the DEM using the burn stream line into DEM tool available from SAGA GIS (CONRAD et al. 2015). This tool adjusts the elevations of DEM grid cells that are coincident with the features of the vector hydrography layer (LINDSAY 2016). The objective is to correct surface drainage patterns derived from the DEM to ensure that they correspond to real flows. Here, the hydrography layer takes into account roads, paths and ditches identified on each date. All roads and paths are considered functional. In other words, all of these infrastructures are considered to intercept and reroute the hydrosedimentary fluxes (Fig. 5D).

3.1.4 Soils and K-Factor

Soil erodibility (K) is a function of soil properties and, more precisely, the grain size of soils. Winegrowers must maintain the soil properties as constant as possible since the definition of Mercurey appellation (1936); as a consequence, we hypothesize that K is roughly constant over time. In Mercurey, a fine-scale map of soil properties has been provided with detailed data regarding grain size (SIGALES 2007). This map has been digitized in a shapefile layer. From grain-size values, we calculated K following the method of WISCHMEIER and SMITH (1978) and RENARD et al. (1997) in eq. 2:

$$K = [(2.1 \times 10^{-4} M^{1.14} (10 - OM) + 3.25 (s - 2) + 2.5 (p - 3)) / 100]$$

where M is the textural factor with $M = (m_{\text{silt}} + m_{\text{vfs}}) * (100 - m_c)$; m_c [%] is the clay fraction content (<0.002 mm); m_{silt} [%] is the silt fraction content (0.002–0.05 mm); m_{vfs} [%] is the very fine sand fraction content (0.05–0.1 mm); and OM [%] is the organic matter content.

3.1.5 R and P-Factors

Factor R (rainfall erosivity) has been recently assessed in Europe (PANAGOS et al. 2015a): it is calculated from 1541 precipitation stations in all European Union (EU) member states and

Switzerland, with temporal resolutions of 5 to 60 min. For the 3 dates, we used the mean of the R factor estimated at the European scale as a constant value: $620 \text{ MJ.Mm.ha}^{-1} \text{ h}^{-1} \text{ yr}^{-1}$.

The P factor is the ratio of soil loss with a specific support practice to the corresponding loss with upslope–downslope tillage (RENARD et al. 1997). These practices seek to reduce erosion susceptibility by hampering runoff emergence and flow concentration. Considering the lack of specific data and without any significant contouring or terracing within crops, it is assumed that P equals 1, an assumption widely accepted in spatial modeling (BAKKER et al. 2008; KOULI et al. 2009; FAGNANO et al. 2012; BORELLI et al. 2014).

3.1.6 GIS modeling and validation

We digitized roads, soil maps and land cover through QGIS to create shapefile layers that have been imported into PCI Geomatica to generate DEM at each date, and into SAGA GIS software to convert all vector data into raster data (Fig. 6). The conversion has been led to integrate all the created layers in the same grid reference, i.e., the grid corresponding to the DEM (resolution = 5 meters); maps of factors LS, K, C are thus raster layers. Following the RUSLE equation (WISCHMEIER and SMITH 1965 and 1978; RENARD et al. 1997), we proceeded to a multiplication between the factor raster layers and the R factor constant $620 \text{ MJ.Mm.ha}^{-1} \text{ h}^{-1} \text{ yr}^{-1}$ (grid calculator within SAGA GIS) to provide an assessment of current erosion susceptibility ($\text{t.ha}^{-1} \text{ yr}^{-1}$). The results are compared with published erosion assessment acquired from field survey in a subcatchment of the area (FRESSARD et al. 2017) to be validated.

3.2 Past erosion susceptibility

3.2.1 Acquisition of primary data

We selected complementary aerial images that represent the different states of the area over time, they should be representative of historical evolution. Additionally, historical images can sometimes be of moderate to poor quality, which is another constraint for multitemporal analysis. The photographs have to be of high visibility (e.g., low cloud cover) and good resolution (at least acquired at the 1/30 000 scale). Furthermore, they should have been acquired during spring when the types of land use are easier to distinguish.

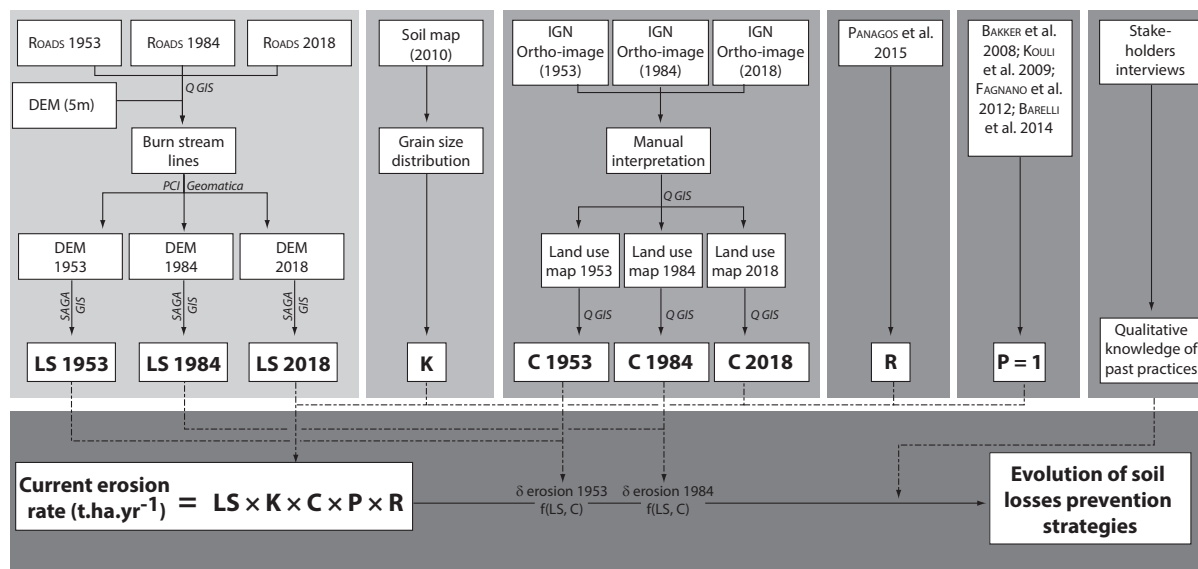


Fig. 6: Methodological framework and GIS implementation workflow. In italics are mentioned the software in which the specific step of the procedure has been implemented.

According to the history of the Mercurey vineyard and the image quality constraint, we selected two complementary dates to document the environmental evolution of Mercurey: 1953 and 1984.

The 1953 aerial photograph (BDOrtho-Historique®, IGN) was taken 7 years after the Second World War. It reveals the initial state at which the spatial extent of the vineyard was at its minimum. Furthermore, such a period corresponds to a stage before the mechanization and the intensification of practices.

The 1984 aerial photograph reveals the stage at which the spatial extent of the vineyard is at its maximum and during which winegrower practices are characterized by mechanization and intensification (frequent tillage, bare soil in interrow vines, intensive chemical weeding, etc.). In Mercurey, the maximal extent of the vineyard occurred earlier than that in other French vineyards (i.e., 1990s in LEGOUY 2014; COSSART et al. 2020) as the 1981 and 1983 flash floods generated stakeholder awareness and a decrease in the surface area dedicated to vineyards.

We also led interviews of 9 stakeholders (8 wine-makers and the mayor of Mercurey) to provide historic qualitative data regarding vineyard environmental issues, helping in the interpretation of our results.

3.2.2 Inferences of past erosion susceptibility

Past C and LS factors were derived from the digitalized land use maps following the same procedure as described above (sections 3.1.2 and 3.1.3). The

RUSLE model is applied here to provide a theoretical comparison of erosion susceptibility during past periods (1953 and 1984) with the current reference frame. Such theoretical application considers that both C and LS factors are evolving through time. We indeed hypothesize that such factors reveal both the land cover evolution (especially agricultural land uses) and the development of a soil erosion management strategy based on the collection of sediments using roads, hedges and ditches (FRESSARD and COSSART 2019). Spatial data focusing on these two parameters can be implemented within a spatiotemporal database to discuss on the coevolution between agricultural practices and erosion susceptibility (Fig. 6). All things being equal, we infer the increase/decrease (in %) of the erosion susceptibility from the current referential frame due to the evolution through time of C factor and LS factor.

4 Results

4.1 Current referential frame of erosion susceptibility

At present the surface area of vines is the dominant type of land use (31%). The other types of land use correspond to forests and grassland, whose surface areas correspond to 28 and 25% of the whole study area, respectively (Fig. 7A). Considering the spatial patterns of land uses at catchment, the mean C factor is currently about 0.19.

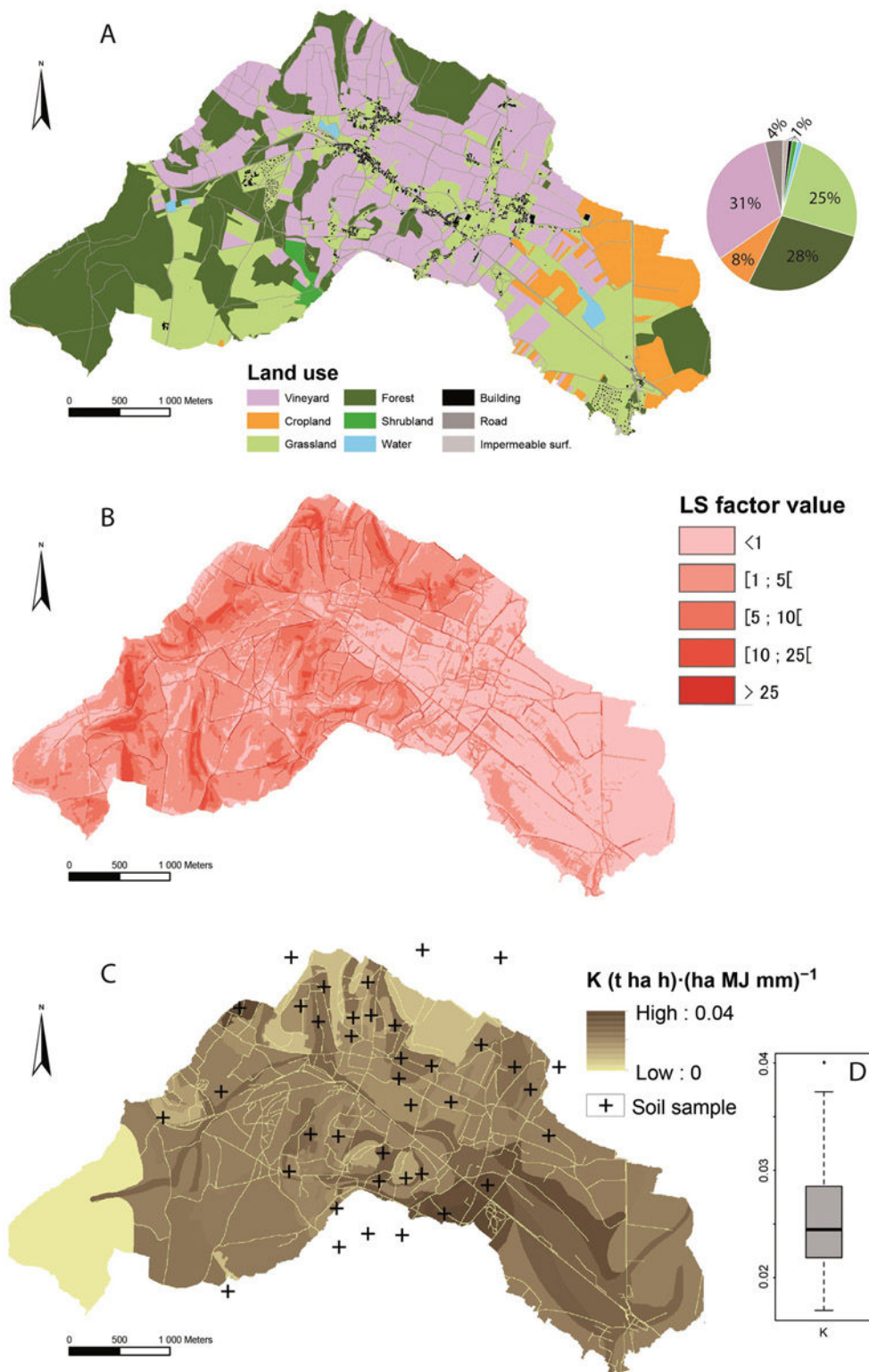


Fig. 7: Primary data to implement RUSLE model in 2018. A: landuse; B: LS factor; C: K factor; D: boxplot of the distribution of the calculated K factors for the 36 soil samples.

In details, we exhibit plots do not exceed 100 meters in length that directly impacts LS factor (Fig. 7B and 8). The latter depends on manmade infrastructures that collect both water and sediments into basins. A precise description in the Vaux area (Fig. 8) shows that basins are connected to a network of lon-

gitudinal collectors (V-shaped roads) located along the main thalwegs of subcatchments. The network aims to concentrate most of the hydrosedimentary flows once they are exported from the vine plots. This longitudinal system is complemented by a transversal network aimed at breaking upstream/down-

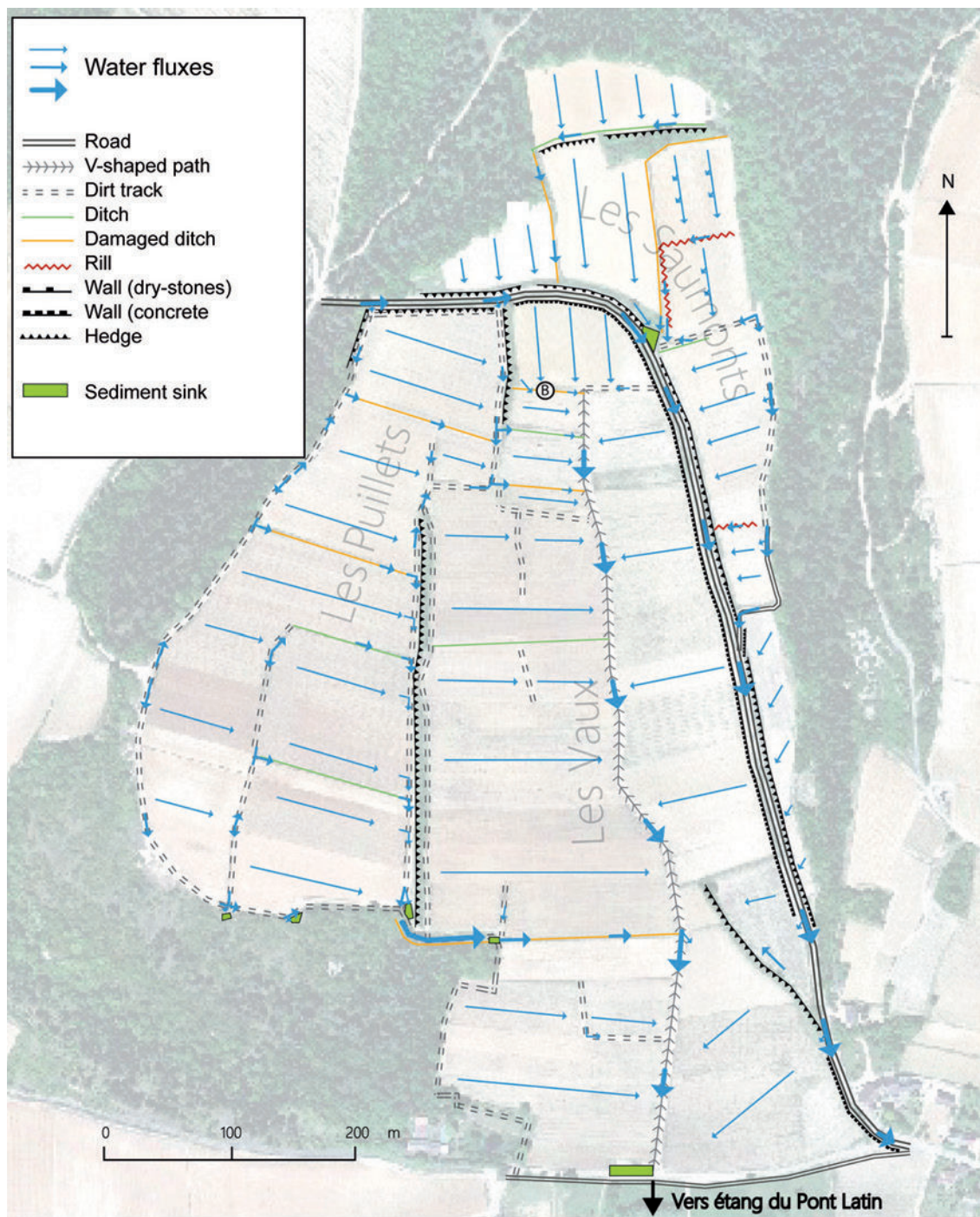


Fig. 8: Inventory of manmade infrastructures built in the 1980s to prevent soil erosion in the Vaux catchment

stream connectivity along hillslopes. Such disconnections are due to transverse tracks that are totally or partially grassed, characterized by a slight counter slope. These infrastructures tend to reduce LS values in vine plots (Fig. 7B). The calculated mean value (4.18) is significantly lower than the value calculated without the impact of man-made infrastructures (7.5). Other types of land use are also affected by the impacts of the artificial routing of water fluxes: parcels of forest and grassland are currently characterized by LS values (3.15, 4.05, respectively) lower than topography-based LS values (3.21, 5.59, respectively).

In Mercurey, K factor values are quite homogeneous. They range from 0.017 to 0.04. The mean is 0.025, the median is 0.024, and the first and third quantiles are 0.022 and 0.028, respectively. This homogeneity in the K factor is directly due to the homogeneity in soil types and OM content (Fig. 7C). Only localized non-calcareous brown soils show higher values on the northwest part of the catchment as well as in the plain area where soils have a higher silt content.

Currently, erosion susceptibility in vineyard is estimated to be $4,909 \text{ t}\cdot\text{yr}^{-1}$ (mean = $12.3 \text{ t}\cdot\text{ha}^{-1}\cdot\text{yr}^{-1}$). In detail, erosion susceptibility ranges from 15 to $42 \text{ t}\cdot\text{ha}^{-1}\cdot\text{yr}^{-1}$ on the hillslopes and 4 to $10 \text{ t}\cdot\text{ha}^{-1}\cdot\text{yr}^{-1}$ next to the valley floor (Fig. 9). The estimated values of erosion susceptibility are about $3 \text{ t}\cdot\text{ha}^{-1}\cdot\text{yr}^{-1}$ for the parcels of forest, approximately $5.7 \text{ t}\cdot\text{ha}^{-1}\cdot\text{yr}^{-1}$ for grasslands and approximately $3 \text{ t}\cdot\text{ha}^{-1}\cdot\text{yr}^{-1}$ for the other types of cultures.

The theoretical estimations of erosion susceptibility in vineyard in 2018 are convergent with recent field surveys realized from stock unearthing measurements (SUMs) in Mercurey (FRESSARD et al. 2017): 8.7 to $17 \text{ t}\cdot\text{ha}^{-1}\cdot\text{yr}^{-1}$. The values are also quite similar to those of other surveys led in Burgundy in the 2000s (Monthelie area, in BRENOT et al. 2008), where soil losses of 15 to $23 \text{ t}\cdot\text{ha}^{-1}\cdot\text{yr}^{-1}$ were measured on moderately steep hillslopes.

4.2 Erosion susceptibility in 1984

In 1984, the landscape of Mercurey was not significantly different from today (Fig. 10A). The surface devoted to the vineyard was dominant at the catchment scale (28%). Grassland surface area also seems similar in 1984 with 2018: it was approximately 25% of the catchment. Conversely, the surface area of forest was lower than today and represented 25% of the total surface area in 1984. The Vaux area is representative of such pattern (Fig. 11). The landscape was indeed homogeneous and characterized by the omnipresence of vines (60% of the Vaux area). At that time vines were located on the whole hillslopes, including both the steepest parts (top) and the lower parts (close to habitations and roads). As a consequence, grassland appeared scarce, while forest cover was only observed on plateaus. We also note the scarcity of hedges, ditches and transverse tracks on hillslope, so that the length of parcels could reach 200 meters (Fig. 11). As

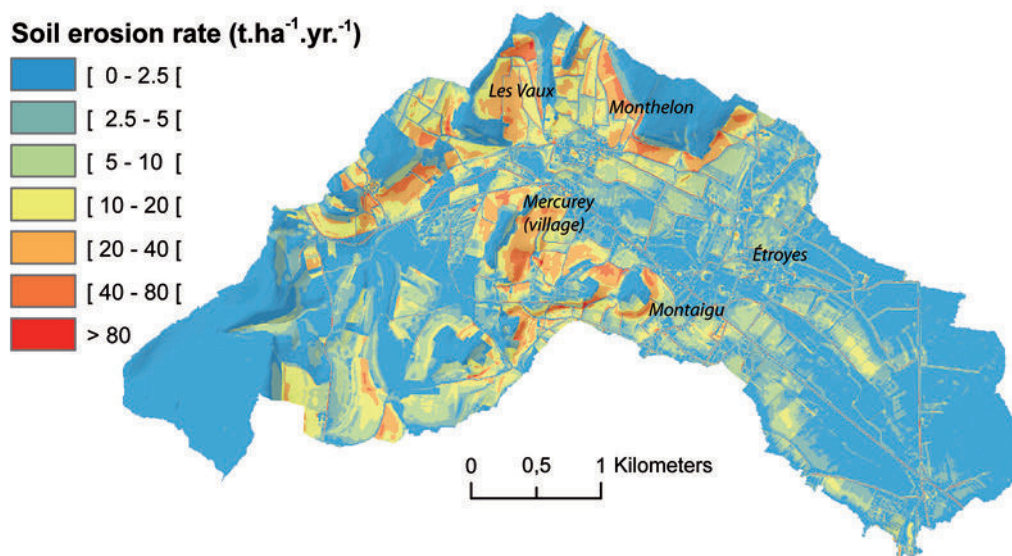


Fig. 9: Map of erosion susceptibility estimated in 2018 from RUSLE model

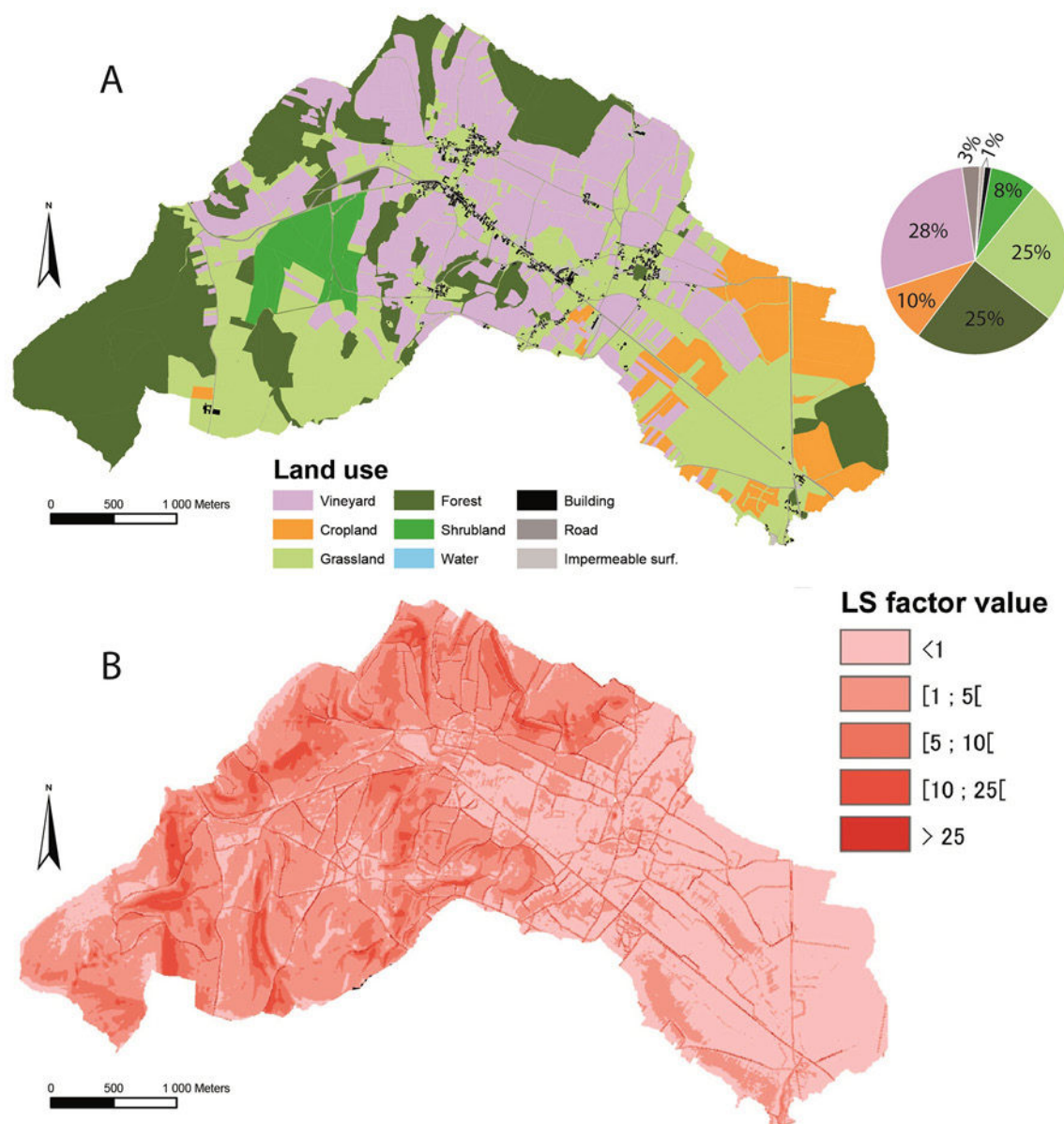


Fig. 10: Land use and LS factor in 1984

a consequence, while the vineyard already covered the main part of hillslopes the LS calculated values were higher than today: 3.22 is calculated at the catchment scale (Fig. 10B and Tab. 2). As the vineyard spread on hillslopes, the mean LS value for vine plots was significantly higher than and reached 7.53 (+3.35). In contrast, as forest was only localized on the plateau in 1984, the mean LS value in forested areas was roughly stable (3.21). The same pattern is highlighted regarding grasslands that are mostly localized on the valley

floor or at the very bottom of hillslopes; the mean LS for grassland plots is approximately 5.59.

Connectivity was thus particularly high in 1984 as no barrier or buffer impeded hydro-sedimentary fluxes along hillslopes. This pattern is confirmed by the interview of local people who lived through the 1980s floods. All things being equal, the 1984 values of LS imply that erosion susceptibility from vines parcels was about +27% higher than the current referential frame.

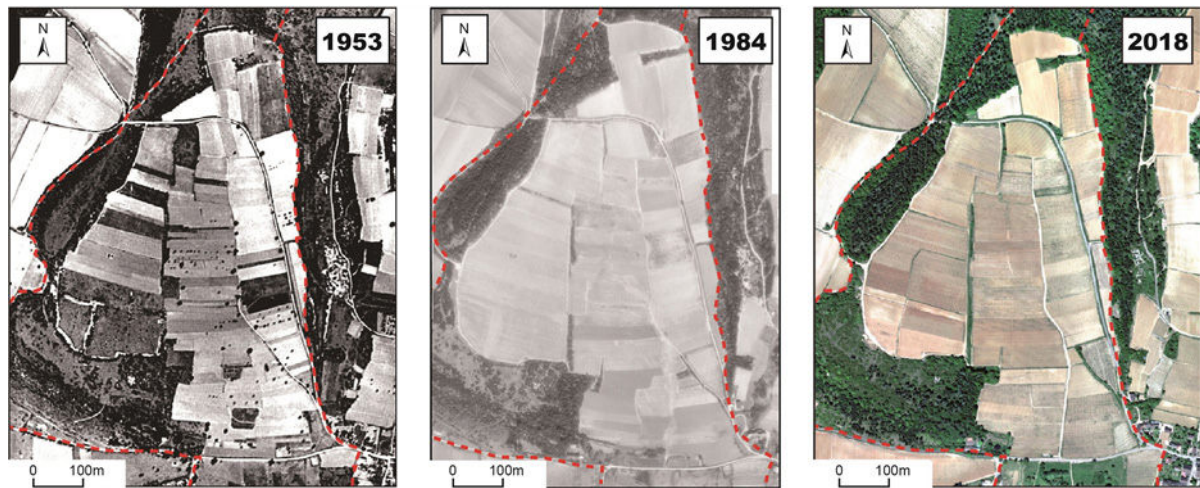


Fig. 11: Focus on Vaux subcatchment, evolution of land use from aerial photographs since 1953 (modified from IGN aerial photographs)

4.3 Erosion susceptibility in 1953

Just after the Second World War, four main types of land use were observed in Mercurey: grassland (38%), forest (25%), vines (22%) and other crops (10%), so vines were not the dominant land use in terms of surface area (Fig. 12A). At the catchment scale, the spatial pattern is as follows: forests are located in the upper parts of hillslopes and plateaus, while grasslands and vines are often combined on hillslopes. In detail, vines are widespread on hillslopes located next to building areas, and conversely, grasslands are widespread in remote areas. Interviewed stakeholders specified that this pattern was classical in Burgundy at that time, as vines require more frequent manual work than grassland (and the associated breeding). From a quantitative point of view, the mean C factor value at the catchment scale was lower than today due to this land use spatial pattern: 0.16 (-0.03).

If we focus at a more local scale on a hillslope where vines were dominant (Vaux area, Fig. 11), the landscape was characterized by contrasting lo-

cal patterns: 42% of the surface area was covered by vines, 35% by forest and 21% by grassland. As observed at the catchment scale, forest covered all the upper parts of the hillslopes. More interesting is the complex assemblage of parcels of vines and parcels of grassland on hillslopes. Landscape spatial patterns created a local land cover diversity reinforced by the presence of many trees within vine parcels. On the one hand, grasslands encourage water infiltration at many locations, especially in the lower parts of the hillslopes. On the other hand, interviews highlight that vine growers previously planted such trees (e.g., *Prunus domestica*, *Malus domestica*, *Prunus Avium*, *Prunus Dulcis*) in vine plots in association with vine growing layering techniques to create a rough surface and more generally to impede surficial runoff. These qualitative data show that farmers were aware of soil erosion prevention issues and had developed active mitigation strategies. A reduction in sediment delivery was thus expected due to land use.

The calculated LS factor in 1953 was approximately 3.22 at the catchment scale, higher than to-

Tab. 2: LS factor values and estimated erosion susceptibility aggregated in specific landscape units

	1953		1984		2018		Total potential soil loss [t/yr]
	LS factor	A [t/ha/yr]	LS factor	A [t/ha/yr]	LS factor	A [t/ha/yr]	
Vines	3.33	9.8	7.53	14.2	4.18	12.3	4909
Grassland	5.71	6.8	5.59	6.6	4.05	5.7	1829
Forest	3.90	1.8	3.21	2.9	3.15	2.7	2032
Other crops	0.13	3.4	0.13	3.1	0.13	3.1	318
Whole area	3.22	6.2	3.22	6.7	3.18	6.6	9152

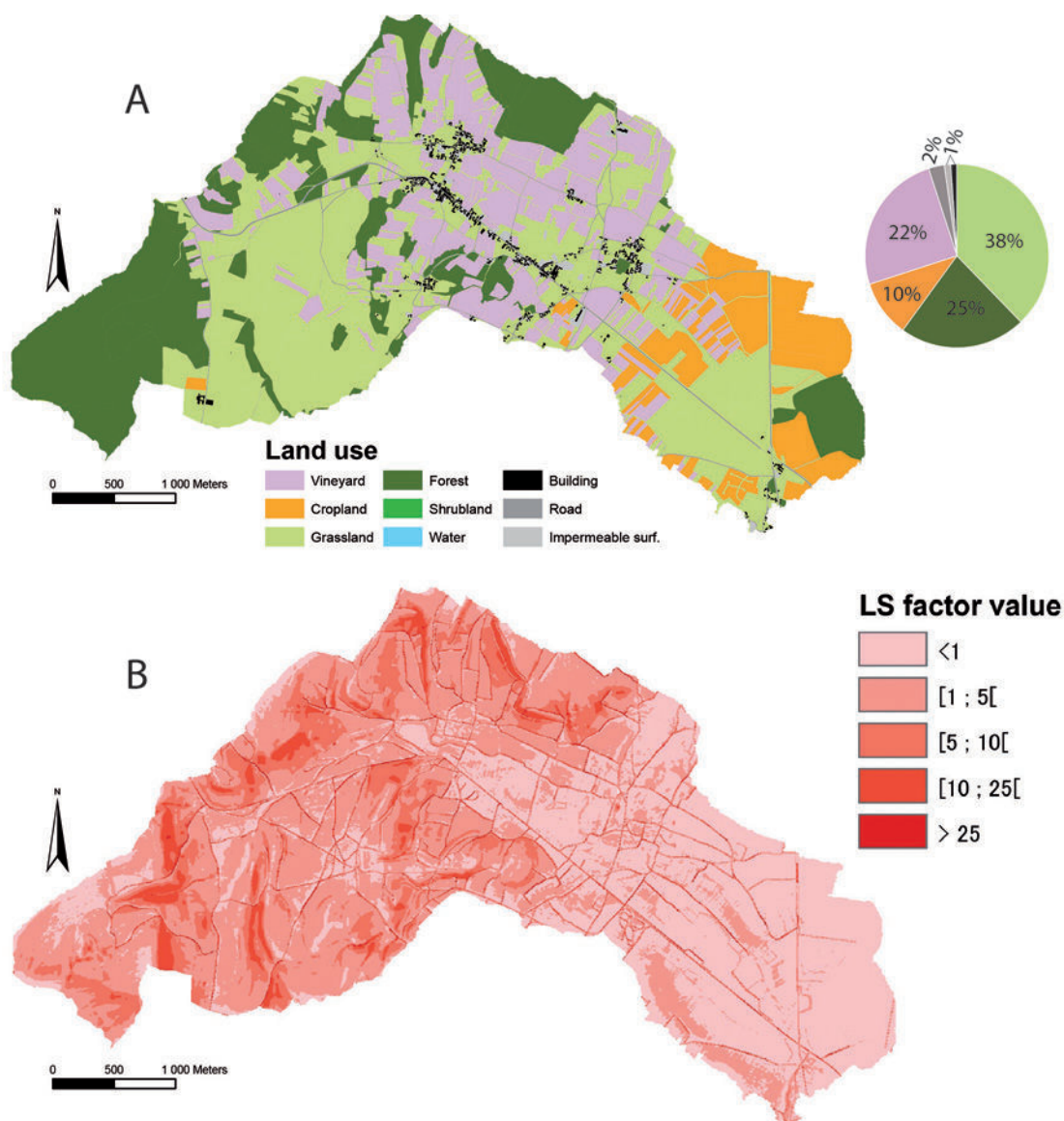


Fig. 12: Land use and LS factor in 1953

day and similar with 1984 values (Tab. 2). This mean value does not reflect the high spatial heterogeneity that existed between the upper parts of hillslopes (about 10) and other areas (Fig. 12B). Values, for instance, range from 1 to 5 on the plateaus and from 0 to 1 on the alluvial plain. In relation to the mosaicking pattern of landscape, the LS value is lower in vine plots (3.33), while it is higher on both parcels of forest (3.9) and grassland (5.71). We thus point out the highest C-factor (vineyard) was compensated for low LS values. All things being equal, it suggests that erosion susceptibility from vines was about -21% below the current referential frame.

5 Discussion

Erosion susceptibility values estimated in 2018 are similar to those of other conventionally cultivated vineyards. The highest theoretical values we estimated on hillslopes (15 to 42 $\text{t}\cdot\text{ha}^{-1}\cdot\text{yr}^{-1}$ in 2018, 15 to 42 $\text{t}\cdot\text{ha}^{-1}\cdot\text{yr}^{-1}$ in 1984) are similar to the results obtained in Aosta (NW Italy), where vine stocks were planted parallel to the slope with bare interrows, and superficial tillage occurred once or twice a year: 15.7 to 31.1 $\text{t}\cdot\text{ha}^{-1}\cdot\text{yr}^{-1}$ (BIDDOCCU et al. 2018). To complement, slightly higher values are observed on steep hillslopes (15 to 30°) in Moselle, where pesticides

and herbicides during the spring and summer are applied to control weeds. In the latter case soil losses range from 32.5 to 63 t·ha⁻¹·yr⁻¹ (RODRIGO-COMINO et al. 2016).

In detail, sediment production is currently probably lower than values estimated in 1980s. Since 1984, the intensification of land use has been compensated for by reparcelling strategies and linear infrastructures that reduced LS factors and thus sediment connectivity on hillslopes (FRESSARD and COSSART 2019). In 1984 the estimated erosion susceptibility was probably about +27 % higher than the current reference level. According to winegrowers interviews, strategies preventing soil losses were in priority applied in high-quality terroirs and in areas where excessive runoff threatened inhabitations during 1980s floods (Fig. 13). As a consequence, the assumption that information about soil erosion in vineyards has often failed to reach farmers (RODRIGO-COMINO 2018) can be here refuted. The severe hydrogeomorphic events (i.e., 1981 and 1983 floods) indeed played a crucial role in raising the awareness of environmental problems, even if the applied strategies are spatially limited.

Before the 1980s peak of erosion, the adequacy of land use with physical settings (especially slope gradient) during the 1950s is revealed by winegrower interviews. Such pattern demonstrates the empirical knowledge acquired by farmers (Fig. 13). While the local economy was almost entirely based on agricultural activities, our theoretical estimations show that erosion susceptibility was indeed moderate (-20% below the current referential frame) for three main reasons. Firstly, avoiding the location of vineyards on the steepest hillslopes was a specific strategy to prevent excessive runoff; vine growers developed activities characterized by lower C values in areas where LS was high. As already demonstrated, such landscape spatial patterns are efficient to prevent soil losses (BAKKER et al. 2008). Secondly, vine growing layering technique before mechanization created a rough soil surface and a chaotic distribution of the vines inside within parcels hampering the organization of runoff processes (DION 1959; MAGNIEN 2002). Third, in the complementary strategy, grassland areas were developed in specific locations to act as buffers in the water and sediment transfers. In detail, grasslands surrounded each inhabited area in the 1950s. As noted by interviewed older farmers (>70 years old), developing land uses characterized by low C values (i.e., grasslands) was easier in the 1950s, as the economic added value of vineyards was lower. Livestock (and associated

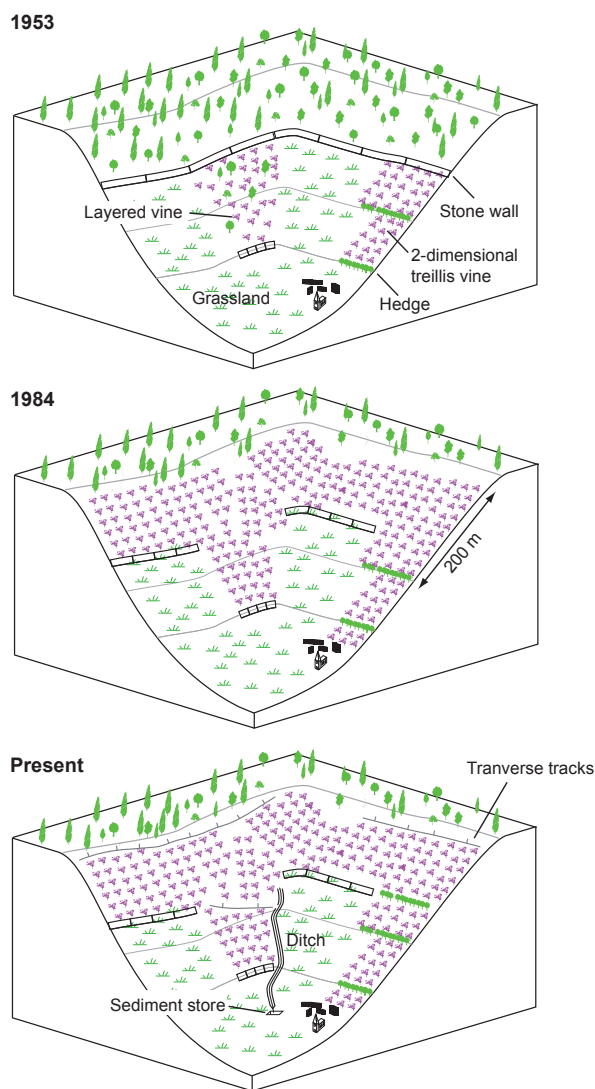


Fig. 13: Evolution of strategies preventing soil losses in Mercurey since 1953

grasslands) was furthermore necessary for food subsistence and to facilitate agricultural work in the fields (MAGNIEN 2002).

More generally, the awareness of soil erosion issues has thus been evidenced in Mercurey vineyards since the mid-20th century and is probably the legacy of the long tradition of soil erosion prevention shown by historical studies (BRENOT 2007; GARCIA 2011; GARCIA et al. 2017). Such a trend seems to have occurred in the whole Burgundy vineyard (GARCIA et al. 2017) in the mid-20th century. More generally the results are convergent with historical works (TAROLLI et al. 2015; GARCIA et al. 2017) that draw the hypothesis that winegrowers implemented strategies to prevent soil erosion at an early stage.

6 Conclusions

According to the RUSLE model implemented here, erosion susceptibility in vineyard is currently estimated to be $4,909 \text{ t.yr}^{-1}$ (mean = $12.3 \text{ t.ha}^{-1}.\text{yr}^{-1}$). In detail, erosion susceptibility ranges from 15 to $42 \text{ t.ha}^{-1}.\text{yr}^{-1}$ on the hillslopes and 4 to $10 \text{ t.ha}^{-1}.\text{yr}^{-1}$ next to the valley floor in Mercurey area. While high, such rate have been reduced since 1984 and severe floods that have facilitated the awareness of local stakeholders. Intensification of land use has been compensated for by reparcelling strategies and linear man-made infrastructures that reduced the sediment connectivity on hillslopes. In 1984 the level of erosion susceptibility in vines parcels was indeed estimated to be +27% higher than the current level. The latter increase was due to vineyards expanding on hillslopes, characterized by long parcels (twice than today). The lack of hedges, ditches and transverse tracks implied a high connectivity and thus a high LS factor. Conversely, in 1953 erosion susceptibility in vines parcels was estimated about -21% below the current referential frame. In the mid-20th century, agricultural practices were adapted with physical settings: activities characterized by high C factors were mostly located in areas where the LS factor was low.

Our results thus demonstrate that stakeholders are aware of soil loss issues even if strategies have changed over time. We now have to test the hypothesis of an early emergence of soil loss mitigation strategies by applying RUSLE models at former stages, such as in the 18th and 19th centuries. These studies can highlight soil prevention models that have been empirically applied in the past by farmers. Although frequently scientifically underestimated, these strategies can help to achieve the objective to ensure that 75% of soils are healthy by 2030 and are able to provide essential ecosystem services (EUROPEAN COMMISSION 2020).

Acknowledgments

We thank the winemakers' association of Mercurey, especially Mr. Duvernay and Mr. Menand, for their interest in our research and for sharing their practical field knowledge in constructive discussions, and A. Potot who provided help in the field. This research was funded by the CNRS, PEPS-THOMIS 2018 program, and by IDEX-Lyon (2015-2016 "connecting" program).

References

- AGRESTE (2018): Recensement Général Agricole (communes de Mercurey et Saint-Martin-sous-Montaigu). Ministère de l'agriculture de l'agroalimentaire et de la forêt, technical report, 2 p.
- BAGAGIOLO, G.; BIDDOCU, M.; RABINO, D. and CAVALLO, E. (2018): Effects of rows arrangement, soil management, and rainfall characteristics on water and soil losses in Italian sloping vineyards. In: *Environmental Research* 166, 690–704. <https://doi:10.1016/j.envres.2018.06.048>
- BAKKER, M. M.; GOVERS, G.; VAN DOORN, A.; QUETIER, F.; CHOUVARDAS, D. and ROUNSEVELL, M. (2008): The response of soil erosion and sediment export to land-use change in four areas of Europe: the importance of landscape pattern. In: *Geomorphology* 98 (3–4), 213–226. <https://doi:10.1016/j.geomorph.2006.12.027>
- BHANDARI, K. P.; ARYAL, J. and DARNASAWSDI, R. (2015): A geospatial approach to assessing soil erosion in a watershed by integrating socio-economic determinants and the RUSLE model. In: *Natural Hazards* 75, 321–342. <https://doi.org/10.1007/s11069-014-1321-2>
- BARRENA-GONZÁLEZ, J.; RODRIGO-COMINO, J.; GYASI-AGYEI, Y.; PULIDO FERNÁNDEZ, M. and CERDÀ, A. (2020): Applying the RUSLE and ISUM in the Tierra de Barros Vineyards (Extremadura, Spain) to estimate soil mobilisation rates. In: *Land* 93 (9), 1–17. <https://doi:10.3390/land9030093>
- BIDDOCU, M.; OPSI, F. and CAVALLO, E. (2014): Relationship between runoff and soil losses with rainfall characteristics and long-term soil management practices in a hilly vineyard (Piedmont, NW Italy). In: *Soil Science and Plant Nutrition* 60 (1), 92–99. <https://doi:10.1080/00380768.2013.862488>
- BIDDOCU, M.; ZECCA, O.; AUDISIO, C.; GODONE, F.; BARMAS, A. and CAVALLO, E. (2018): Assessment of long-term soil erosion in a mountain vineyard, Aosta Valley (NW Italy). In: *Land Degradation Development*, 29, 617–629. <https://doi.org/10.1002/ldr.2657>
- BLAVET, D.; DE NONI, G.; LE BISSONNAIS, Y.; LEONARD, M.; MAILLO, L.; LAURENT, J. Y.; ASSELINE, J.; LEPRUN, J. C.; ARSHAD, M. A. and ROOSE, E. (2009): Effect of land use and management on the early stages of soil water erosion in French Mediterranean vineyards. In: *Soil and Tillage Research* 106 (1), 124–136. <https://doi.org/10.1016/j.still.2009.04.010>
- BORRELLI, P.; MÄRKER, M.; PANAGOS, P. and SCHÜTT, B. (2014): Modeling soil erosion and river sediment yield for an intermountain drainage basin of the Central Apennines, Italy. In: *Catena* 114, 45–58. <https://doi:10.1016/j.catena.2013.10.007>
- BORRELLI, P.; VAN OOST, K.; MEUSBURGER, K.; ALEWELL, C.; LUGATO, E. and PANAGOS, P. (2018): A step towards a

- holistic assessment of soil degradation in Europe: coupling on-site erosion with sediment transfer and carbon fluxes. In: *Environmental Research* 161, 291–298. <https://doi.org/10.1016/j.envres.2017.11.009>
- BRENOT, J. (2007): Quantification de la dynamique sédimentaire en contexte anthropisé. L'érosion des versants viticoles de Côte d'Or. PhD thesis. Bourgogne.
- BRENOT, J.; QUIQUEREZ, A.; PETIT, C. and GARCIA, J.-P. (2008): Erosion rates and sediment budgets in vineyards at 1-m resolution based on stock unearthing (Burgundy, France). In: *Geomorphology* 100, 345–355. <https://doi.org/10.1016/j.geomorph.2008.01.005>
- CERDAN, O.; POESEN, J.; GOVERS, G.; SABY, N.; LE BISSONNAIS, Y.; GOBIN, A.; VACCA, A.; QUINTON, J.; AUERSWALD, K. and KLIK, A. (2006): Sheet and rill erosion. In: *Soil Erosion in Europe*, 501–513. <https://doi.org/10.1002/0470859202.ch38>
- CIAMPALINI, R.; FOLLAIN, S. and LE BISSONNAIS, Y. (2012): LandSoil: a model for the analysis of the impact of erosion on agricultural landscape evolution. In: *Geomorphology* 175–176, 25–37. <https://doi.org/10.1016/j.geomorph.2012.06.014>
- CONRAD, O.; BECHTEL, B.; BOCK, M.; DIETRICH, H.; FISCHER, E.; GERLITZ, L.; WEHBERG, J.; WICHMANN, V. and BÖHNER, J. (2015): System for Automated Geoscientific Analyses (SAGA) v. 2.1.4. In: *Geoscientific Model Development* 8, 1991–2007. <https://doi.org/10.5194/gmd-8-1991-2015>
- COSSART, E.; PIC, J.; LE GUEN Y. and FRESSARD, M. (2020): Spatial patterns of vineyard abandonment and related land use transitions in Beaujolais (France): a multi-scale approach. In: *Sustainability* 12, 4695. <https://doi.org/10.3390/su12114695>
- DAVID, M.; FOLLAIN, S.; CIAMPALINI, R.; LE BISSONNAIS, Y.; COUTURIER, A. and WALTER, C. (2014): Simulation of medium-term soil redistributions for different land use and landscape design scenarios within a vineyard landscape in Mediterranean France. In: *Geomorphology* 214, 10–21. <https://doi.org/10.1016/j.geomorph.2014.03.016>
- DESMET, P. J. J. and GOVERS, G. (1996): A GIS procedure for automatically calculating the USLE LS factor on topographically complex landscape units. In: *Journal of Soil and Water Conservation* 51 (5), 427–433
- DION, R. (1959): Histoire de la vigne et du vin en France. Paris.
- EUROPEAN COMMISSION (2020): Caring for soils is caring for life. Publications of the European Union. <https://doi.org/10.2777/918775>
- FAGNANO, M.; DIODATO, N.; ALBERICO, I. and FIORENTINO, N. (2012): An overview of soil erosion modelling compatible with RUSLE approach. In: *Rendiconti Lincei* 23 (1), 69–80. <https://doi.org/10.1007/s12210-011-0159-8>
- FOLLAIN, S.; CIAMPALINI, R.; COULOUMA, G.; CRABIT, A. and GARNIER, F. (2012): Effects of redistribution processes on rock fragment variability within a vineyard topsoil in Mediterranean France. In: *Geomorphology* 175–176, 45–53. <https://doi.org/10.1016/j.geomorph.2012.06.017>
- FRESSARD, M. and COSSART, E. (2019): A graph theory tool for assessing structural sediment connectivity: development and application in the Mercurey vineyards (France). In: *Science of The Total Environment* 651 (2), 2566–2584. <https://doi.org/10.1016/j.scitotenv.2018.10.158>
- FRESSARD, M.; COSSART, É.; ALAMI, C.; BRUN, G.; POTOT, A.; LEJOT, J.; BOULET, R. and CHRISTOL, A. (2017): Casser la connectivité hydrosédimentaire pour gérer la ressource en sol: cas du vignoble de Mercurey (Bourgogne). In: *Géomorphologie: Relief, Processus, Environnement*. <https://doi.org/10.4000/geomorphologie.11865>
- GANASRI, B. P. and RAMESH, H. (2016): Assessment of soil erosion by RUSLE model using remote sensing and GIS - A case study of Nethravathi Basin. In: *Geoscience Frontiers* 7 (6), 953–961. <https://doi.org/10.1016/j.gsf.2015.10.007>
- GARCIA, J.-P. (2011): Les sols viticoles de Bourgogne : élaboration naturelle et construction humaine. In: *Revue des Oenologues et des Techniques Vitivinicoles et Oenologiques*, 62–64
- (2018): Le vin et le lieu. In: *Crescentis: Revue internationale d'histoire de la vigne et du vin* 1–2.
- GARCIA, J.-P.; GRILLON, G. and LABBÉ, T. (2017): Terroirs, climats ... ou le vin et le lieu en Bourgogne. In: *Terroirs et climats*, 42–48
- GARCIA, J.-P.; LABBÉ, T. and QUIQUEREZ, A. (2018): La préservation et la pérennisation des sols viticoles en Bourgogne du Moyen Âge à nos jours. In: PÉRARD, J. and WOLIKOW, C. (eds.): *Quelle durabilité en vignes et en cave*. Clos Vougeot, 51–65.
- GRIMM, M.; JONES, R. J.; RUSCO, E. and MONTANARELLA, L. (2003): Soil erosion risk in Italy: a revised USLE approach. Luxembourg.
- GRIVOT, F. (1954): Les vins de la côte chalonaise. In: *L'information géographique* 18 (1), 32–37. <https://doi.org/10.3406/ingeo.1954.1351>
- HENGL, T. (2006): Finding the right pixel size. In: *Computers & geosciences* 32 (9), 1283–1298. <https://doi.org/10.1016/j.cageo.2005.11.008>
- JAHUN, B. G.; IBRAHIM, R.; DLAMINI, N. S. and MUSA, S. M. (2015): Review of soil erosion assessment using RUSLE model and GIS. In: *Journal of Biology, Agriculture and Healthcare* 5 (9), 36–47.
- KINNELL, P. I. A. (2005): Alternative approaches for determining the USLE-M slope length factor for grid cells. In: *Soil Science Society of America Journal* 69 (3), 674–680. <http://soil.scijournals.org/cgi/content/full/69/3/674>

- (2010): Event soil loss, runoff and the Universal Soil Loss Equation family of models: a review. In: *Journal of Hydrology* 385, 384–397. <https://doi.org/10.1016/j.jhydrol.2010.01.024>
- LI, J. and WONG, D. W. (2010): Effects of DEM sources on hydrologic applications. In: *Computers, Environment and Urban Systems* 34 (3), 251–261. <https://doi.org/10.1016/j.compenvurbsys.2009.11.002>
- KOULLI, M.; SOUPIOU, P. and VALLIANATOS, F. (2009): Soil erosion prediction using the Revised Universal Soil Loss Equation (RUSLE) in a GIS framework, Chania, Northwestern Crete, Greece. In: *Environmental Geology* 57 (3), 483–497. <https://doi.org/10.1007/s00254-008-1318-9>
- LABBÉ, T. and GARCIA, J.-P. (2019): Amendement et renouvellement des sols dans la viticulture bourguignonne aux XIV^e et XV^e siècles. In: Conesa, M. and Poirier, N. (eds.): *Fumiers ! Ordures ! Gestion et usage des déchets dans les campagnes de l'Occident médiéval et moderne*, Actes des XXXVIII^es Journées internationales d'histoire de l'abbaye de Flaran, 14 et 15 octobre 2016. Toulouse, 69–85.
- LAMMOGLIA, A.; LETURCQ, S. and DELAY, E. (2018): Le modèle VitiTerroir pour simuler la dynamique spatiale des vignobles sur le temps long (1836–2014). In: *Cybergeo: European Journal of Geography* 863. <https://doi.org/10.4000/cybergeo.29324>
- LARUE, J.-P.; MAHOUE, J.-P. and MONNIER, J. (1999): Erosion in cultivated soils and river morphodynamics: the example of the tortue basin (Sarthe, France). In: *Geodinamica Acta* 12 (2), 57–70. <https://doi.org/10.1080/09853111.1999.11105331>
- LARUE, J.-P. (2001): Runoff and interrill erosion on sandy soils under cultivation in the western Paris basin: mechanisms and an attempt at measurement. In: *Earth Surface Processes and Landforms* 26, 971–989. <https://doi.org/10.1002/esp.238>
- LEDERMANN, T.; HERWEG, K.; LINIGER, H. P.; SCHNEIDER, F.; HURNI, H. and PRASUHN, V. (2010): Applying erosion damage mapping to assess and quantify off-site effects of soil erosion in Switzerland. In: *Land Degradation Development* 21, 353–366. <https://doi.org/10.1002/ldr.1008>
- LEGOUY, F. (2014): La géohistoire de l'espace viticole français sur deux siècles (1808–2010): plusieurs cycles viticoles décryptés. In: *Espaces Temps* 2014, 1–14. <https://www.espacestems.net/articles/la-geohistoire-de-l-espace-viticole-francais/>
- LINDSAY, J. B. (2016): The practice of DEM stream burning revisited. In: *Earth Surface Processes and Landforms* 41, 658–668. <https://doi.org/10.1002/esp.3888>
- MAGNIEN, C. (2002): *Vignerons à Gevrey-Chambertin: 1847–1952*. Paris.
- MÄRKER, M.; ANGELI, L.; BOITAI, L.; COSTANTINI, R.; FERRARI, R.; INNOCENTI, L. and SICILIANO, G. (2008): Assessment of land degradation susceptibility by scenario analysis: a case study in Southern Tuscany, Italy. In: *Geomorphology* 93, 120–126. <https://doi.org/10.1016/j.geomorph.2006.12.020>
- MÉRIAUX, S.; CHRETIEN, J.; VERMI, P.; LENEUF, N. (1981): La Cote viticole. Ses sols et ses crus. In: *Bulletin Scientifique de Bourgogne* 34, 17–40.
- MOORE, I. D.; GRAYSON, R. B. and LADSON, A. R. (1991): Digital terrain modelling: a review of hydrological, geomorphological, and biological applications. In: *Hydrological Processes* 5 (1), 3–30. <https://doi.org/10.1002/hyp.3360050103>
- PANAGOS, P.; BALLABIO, C.; BORRELLI, P.; MEUSBURGER, K.; KLIK, A.; ROUSSEVA, S.; PERČEC TADIĆ, M.; MICHAELIDES, M.; HRABALÍKOVÁ, M.; OLSEN, P.; AALTO, J.; LAKATOS, M.; RYMSZEWCZ, A.; DUMITRESCU, A.; BEGUERÍA, S. and ALEWELL, C. (2015a): Rainfall erosivity in Europe. In: *Science of The Total Environment* 511, 801–814. <https://doi.org/10.1016/j.scitotenv.2015.01.008>
- PANAGOS, P.; BORRELLI, P.; MEUSBURGER, K.; ALEWELL, C.; LUGATO, E. and MONTANARELLA, L. (2015b): Estimating the soil erosion cover-management factor at the European scale. In: *Land Use Policy* 48, 38–50. <https://doi.org/10.1016/j.landusepol.2015.05.021>
- PAROISSIEN, J.-B.; LAGACHERIE, P. and LE BISSONNAIS, Y. (2010): A regional-scale study of multidecadennial erosion of vineyard fields using vine-stock unearthing–burying measurements. In: *Catena* 82, 159–168. <https://doi.org/10.1016/j.catena.2010.06.002>
- PONTE LIRA, C.; TABORDA, R.; CARAPUÇO, A. M. and ANDRADE, C. (2012): Adding a temporal dimension to the RUSLE model: application to the Portuguese west coast. *International Geoscience and Remote Sensing Symposium (IGARSS)*. <https://doi.org/10.1109/IGARSS.2012.6352710>
- PROSDOCIMI, M.; CERDÀ, A. and TAROLLI, P. (2016): Soilwater erosion on Mediterranean vineyards: a review. In: *Catena* 141, 1–21. <https://doi.org/10.1016/j.catena.2016.02.010>
- QUIQUEREZ, A.; BRENOT, J.; GARCIA, J. P. and PETIT, C. (2008): Soil degradation caused by a high intensity rainfall event: implications for medium-term soil sustainability in Burgundian vineyards. In: *Catena* 73 (1), 89–97. <https://doi.org/10.1016/j.catena.2007.09.007>
- RACLOT, D.; LE BISSONNAIS, Y.; LOUCHART, X.; ANDRIEUX, P.; MOUSSA, R. and VOLTZ, M. (2009): Soil tillage and scale effects on erosion from fields to catchment in a Mediterranean vineyard area. In: *Agriculture, Ecosystems & Environment* 134, 3–4, 201–210. <https://doi.org/10.1016/j.agee.2009.06.019>
- RENARD, K. G.; FOSTER, G. R. and WEESIES, G. A. (1997): *Predicting soil erosion by water: a guide to conservation planning with the Revised Universal Soil Loss Equation (RUSLE)*. Washington, D.C.

- RANZI, R.; LE, T. H.; RULLI, M. C. (2012): A RUSLE approach to model suspended sediment load in the Lo river (Vietnam): effects of reservoirs and land use changes. In: *Journal of Hydrology* 422–423, 17–29. <https://doi.org/10.1016/j.jhydrol.2011.12.009>
- REULIER, R.; DELAHAYE, D. and VIEL, V. (2019): Agricultural landscape evolution and structural connectivity to the river for matter flux, a multi-agents simulation approach. In: *Catena* 174, 524–535. <https://doi.org/10.1016/j.catena.2018.11.036>
- RODRIGO-COMINO, J. (2018): Five decades of soil erosion research in “terroir”. The State-of-the-Art. In: *Earth-Science Reviews* 179, 436–447. <https://doi.org/10.1016/j.earscirev.2018.02.014>
- RODRIGO COMINO, J.; QUIQUEREZ, A.; FOLLAIN, S.; RACLOT, D.; LE BISSONNAIS, Y.; CASALI, J. and RIES, J. B. (2016): Soil erosion in sloping vineyards assessed by using botanical indicators and sediment collectors in the Ruwer-Mosel valley. In: *Agriculture, Ecosystems & Environment* 233, 158–170. <https://doi.org/10.1016/j.agee.2016.09.009>
- SCHULZE, R. (2000): Transcending scales of space and time in impact studies of climate and climate change on agro-hydrological responses. In: *Agriculture, Ecosystems and Environment* 82, 185–212. [https://doi.org/10.1016/S0167-8809\(00\)00226-7](https://doi.org/10.1016/S0167-8809(00)00226-7)
- SHIT, P. K.; NANDI, A. S. and BHUNIA, G.S. (2015): Soil erosion risk mapping using RUSLE model on jhargram subdivision at West Bengal in India. In: *Modeling Earth Systems and Environment* 1, 28. <https://doi.org/10.1007/s40808-015-0032-3>
- SIGALES, (2007): Les terroirs de l'appellation Mercurey. Internal report of the union of the Mercurey winemakers. Mercurey.
- TAROLLI, P.; SOFIA, G.; CALLIGARO, S.; PROSDOCIMI, M.; PRETI, F. and DALLA FONTANA, G. (2015): Vineyards in terraced landscapes: new opportunities from Lidar data. In: *Land Degradation and Development* 26, 92–102. <https://doi.org/doi:10.1002/ldr.2311>
- VAUDOUR, E., (2002): The quality of grapes and wine in relation to geography: notions of terroir at various scales. In: *Journal of Wine Research* 13, 117–141. <https://doi.org/10.1080/0957126022000017981>
- WISCHMEIER, W. H. and SMITH, D. D. (1965): Predicting rainfall erosion losses from cropland east of the Rocky Mountains. United States Department of Agriculture, Handbook no. 282. Washington, D.C.
- (1978): Predicting rainfall erosion losses: a guide to conservation planning. United States Department of Agriculture, Handbook no. 537. Washington, D.C.

Authors

Prof. Dr. Étienne Cossart
 Dr. Brian Chaize
 Université de Lyon - Jean Moulin (Lyon 3)
 UMR 5600 CNRS – Environnement Ville Société
 1C avenue des Frères Lumière
 CS 78242
 F-69372 LYON
 CEDEX 08France
 etienne.cossart@univ-lyon3.fr

Dr. Mathieu Fressard
 UMR 5600 CNRS – Environnement Ville Société
 5 avenue Pierre Mendès-France
 F-69676 BRON Cedex
 France